

Development of Injectable and Biodegradable Needle-Type Starch Implant for Effective Intratumoral Drug Delivery and Distribution

Changkyu Lee

Department of Biopharmaceutical Engineering, Division of Chemistry and Biotechnology, Dongguk University, Gyeongju, Korea

Correspondence: Changkyu Lee, Email leeck30421@dongguk.ac.kr

Introduction: Compared to intravenous administration, intratumoral drug administration enables the direct delivery of drugs to tumors and mitigates the systemic absorption of drugs and associated drug-induced side effects. However, intratumoral drug administration presents several challenges. The high interstitial fluid pressure (IFP) of the tumor prevents the retention of drugs within the tumor; thus, significant amounts of the drugs are absorbed systemically through the bloodstream or delivered to non-target sites. To solve this problem, in this study, a drug-enclosed needle-type starch implant was developed that can overcome IFP and remain in the tumor.

Methods: Injectable needle-type starch implants (NS implants) were prepared by starch gelatinization and drying. The structure, cytotoxicity, and anticancer effects of the NS implants were evaluated. Biodistribution of NS implants was evaluated in pork (in vitro), dissected liver (ex vivo), and 4T1 tumors in mice (in vivo) using a fluorescence imaging device.

Results: The prepared NS implants exhibited a hydrogel structure after water absorption. NS implants showed effective cytotoxicity and anticancer effects by photothermal therapy (PTT). The NS implant itself has sufficient strength and can be easily injected into a desired area. In vivo, the NS implant continuously delivered drugs to the tumor more effectively and uniformly than conventional hydrogels and solutions.

Conclusion: This study demonstrated the advantages of needle-type implants. An injectable NS implant can be a new formulation that can effectively deliver drugs and exhibit anticancer effects.

Keywords: starch, implant, photothermal therapy, intratumoral drug administration, uniform drug distribution

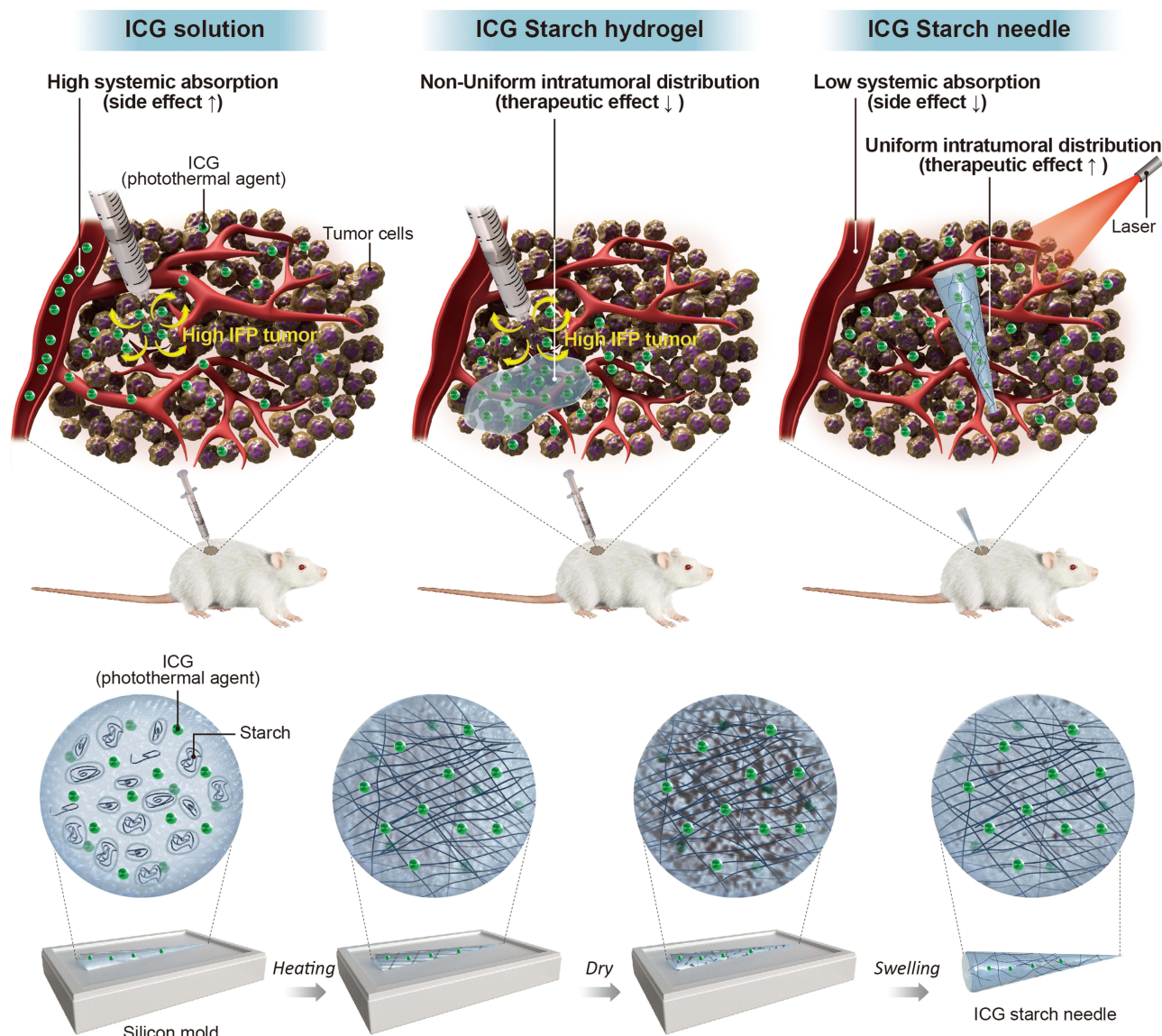
Introduction

Cancer, one of the leading causes of death worldwide, contributes to approximately 8 million deaths each year.¹ PTT is an effective treatment that kills cancer cells by converting light into heat.^{2,3} The ultimate goal of PTT is to effectively kill cancer cells without damaging normal cells. To achieve this, it is important to accumulate high concentrations of photothermal agents in tumors. Indocyanine green (ICG) is an FDA-approved near-infrared (NIR) dye used in a variety of diagnostic applications. It has a photothermal conversion ability that effectively absorbs NIR rays and converts them into heat. Owing to its rapid clearance and low tumor-targeting ability, ICG is delivered to tumors in small amounts by intravenous injection and has a limited therapeutic effect. To overcome the limitations of rapid clearance and low tumor-targeting ability of ICG, various drug delivery systems have been developed using nanoparticles.^{4,5} Nanoparticles can accumulate in tumors owing to their enhanced permeability and retention effects. However, recent studies have demonstrated that intravenous administration of nanoparticles also has limited tumor-targeting efficiency. Although nanoparticles exhibit better tumor-targeting efficiency than drugs alone, only 0.7% of nanoparticles can be delivered to the tumor, due to various barriers, such as the extracellular matrix and interstitial fluid pressure (IFP).^{6,7}

One method for overcoming this limitation is intratumoral injection. The recent development of various endoscopes and surgeries has enabled easy access to tumors and intratumoral drug injection.^{8,9} Intratumoral drug injections deliver



Graphical Abstract



the drug directly into the tumor. Hence, compared with intravenous injection, intratumoral injection is associated with higher drug delivery and fewer systemic side effects.^{10,11} However, a high IFP in solid tumors can be an obstacle to conventional intratumoral (IT) injections of drugs. The IFP of the tumor forms a pressure gradient that is high in the center and low in the periphery. As a result, a drug administered to a tumor through IT injection does not stay in the tumor core due to the pressure gradient but is pushed out or leaked throughout the body.^{12,13} To address this issue, various methods have been developed to reduce the amount of drug absorbed into the blood vessels and enhance the continuous release of the drug using different drug delivery systems, such as hydrogels, microneedles, and implant.^{14–16} However, the hydrogel may not be injected at the target location inside the tumor because of the high internal pressure and may be easily transferred to non-target sites.^{17–19} Additionally, the drug may not spread throughout the tumor but only within the vicinity of the hydrogel.

Microneedle patches and implants are solid formulations; unlike fluid hydrogels or liquids, they are not pushed out by the IFP after intratumoral administration and can remain at the injected site within the tumor.²⁰ A microneedle patch is a

transdermal patch made of small needles, and unlike conventional needles, it can effectively deliver drugs to the dermis without pain. However, microneedles can deliver drugs only to the tumor surface, which limits their use. Implants have a high therapeutic effect because they contain formulations that can continuously release drugs from inside the tumor.²¹ The GLIADEL WAFER, approved for brain cancer treatment, is such an implant anticancer product.²² However, implants require surgical procedures such as incisions, which are associated with side effects such as infection, pain, and bleeding.²³ To address this problem, an easily injectable NS implant was prepared in this study. An NS implant is an implant with strong rigidity for injection and is manufactured in the form of a needle. The NS implant can be delivered to the target area in easily accessible cancers, such as breast cancer, through a simple injection and without the need for special techniques. In the case of other cancers, after accessing the tumor using an endoscope, an NS implant can be easier to inject into the tumor than conventional implants or hydrogels. Subsequently, the NS implant continuously releases the drug from inside the tumor, which enables the uniform distribution of large amounts of the drug throughout the tumor. These results indicate that NS implants are more convenient, safe, and effective than conventional IT injections.

Starch is an inexpensive, readily available, biodegradable and biocompatible biopolymer. Starch has been used for the development of various biomedical materials such as nanoparticles, hydrogels, and stents.^{24,25} Heating disrupts the crystalline structure of starch and leads to gelatinization of the starch solution. Disrupted starch structure can absorb moisture to generate a stable three-dimensional hydrogel network. During the drying process, starch recrystallizes through retrogradation, which results in the production of NS implants that exhibit optimal rigidity for injection.^{25,26} The industrial production of NS implants is simple, reproducible, and cost effective.

This study demonstrated that biodegradable NS could be developed as an effective drug delivery system for cancer treatment. The intratumoral delivery of drug-loaded NS implants resulted in effective growth inhibitory effects against cancer. In this study, novel drug-loaded NS-implants were developed for effective and easy intratumoral injections.

Materials and Methods

Materials

Corn starch and potato starch were purchased from Daejung Chemicals (Gyeonggi-do, Korea) Indocyanine green (ICG) was purchased from Sigma-Aldrich (St. Louis, MO, USA and Tokyo Chemical Industry, Tokyo, Japan, respectively). The LIVE/DEAD viability/cytotoxicity kit was purchased from Thermo Fisher Scientific (Waltham, MA, USA). 4T1 cells were purchased from the American Type Culture Collection. Dulbecco's modified Eagle's medium and fetal bovine serum (FBS) were purchased from Gibco (Dublin, Ireland). All other reagents were obtained from Sigma-Aldrich, unless otherwise specified.

Animals

BALB/c mice (male, 6 weeks old) were purchased from Orient Bio. All mice were maintained under specific pathogen-free conditions. All in vivo experiments were performed in accordance with the guidelines and approval of the Institutional Animal Care and Use Committee of Dongguk University, Gyeongju.

Preparation of Cyanine 5 (Cy5)-NS Implant, ICG-NS Implant, and Cy5-Starch Hydrogel

NS implants were prepared using silicone molds with needle holes. Corn starch and potato starch were mixed in a ratio of 8:2 (starch mixture). For biodistribution analysis, Cy5 loaded NS implant (Cy5-NS implants) were prepared by mixing 100 μ g Cy5, 200 μ L distilled water (DW), and 200 mg starch mixture and pouring 40 mg of the mixture into a silicone mold (10 μ g Cy5 per needle). The mixture was incubated for 20 min at 80 °C above the gelatinization temperature, dried at 25 °C for 1 d, and stored in a refrigerator. For PTT, the ICG-loaded NS implant (ICG-NS implant) was similarly prepared by mixing 2 mg ICG, 200 μ L DW, and 200 mg starch. For comparison of NS implants and hydrogels, a Cy5-starch hydrogel was prepared by mixing 100 μ g of Cy5, 200 μ L of distilled water (DW), and 200 mg of starch mixture and pouring 40 mg in a 1.5 mL

Eppendorf tube (10 μg Cy5 per hydrogel). The starch hydrogel was softened in 1 mL of 10 mM phosphate-buffered saline (PBS, pH 7.4) for 1 h and then immediately injected and used.

Characterization of NS Implant

To analyze the size and shape of the ICG-NS and Cy5-NS implants, the dried NS and NS implants suspended in 10 mM PBS (pH 7.4) for 4 h were photographed. The swelling profile was analyzed by incubating 10 mg of ICG-NS and Cy5-NS implants in 10 mM PBS (pH 7.4) at 37 °C for pre-defined time points (30, 60, 120, and 240 min). The samples were retrieved, wiped with a filter paper, and weighed. The ICG-NS and Cy5-NS implants obtained immediately after gelatinization were dried and incubated in 10 mM PBS (pH 7.4) for 4 h and then lyophilized and subjected to SEM analysis. NS implants were injected into a dissected tumor to demonstrate that they could be injected without the need for special instrumentation.

Release Profile of ICG-NS Implant

To evaluate the release of ICG-NS implants, ICG-NS implants were placed in 10 mL of 10 mM PBS (pH 7.4) and 10 mM PBS (pH 7.4) containing 1 mg/mL glucoamylase and were incubated at 37 °C. After 4 h of incubation, the samples were irradiated with and without a near-infrared (NIR) laser for 5 min (1 W/cm²). Samples were collected at set times (0, 2, 4, 8, 24, 48, 72h). The amount of ICG released was evaluated by measuring absorbance (ICG, 808 nm).

In vitro Cytotoxicity

The cytotoxicity of the ICG-NS implants was evaluated using MTT and live/dead assays.^{19,20} Briefly, the cytotoxic and photothermal effects of ICG-NS implants were analyzed using the (3-[4,5-dimethylthiazol-2-yl]-2,5 diphenyl tetrazolium bromide) (MTT) assay. 4T1 cells (10⁵ cells/mL) were cultured in a 96-well plate for 24 h (100 μL /well). Next, the cells were incubated with a fragment of NS implant (starch 2 mg) or ICG-NS implant (starch 2 mg; ICG 20 μg) for 12 h and irradiated with an NIR laser for 5 min (1 W/cm²). Cytotoxicity was assessed using an MTT assay 24 h after irradiation.

A live/dead assay kit was used to evaluate the death and viability of 4T1 cells. 4T1 cells (10⁵ cells/mL) were cultured in an 8-well chamber (Ibidi, Martin-Sried, Germany) for 24 h (100 μL /well). Next, the cells were incubated with a fragment of NS implant (starch 1 mg) or ICG-NS implant (starch 1 mg; ICG 10 μg) for 12 h and irradiated with a near-infrared (NIR) laser for 5 min (1 W/cm²).

After 24 h, live cells were stained with calcein-AM (live cells stained green), and dead cells were stained with ethidium homodimer-1 (dead cells stained red). The excitation/emission wavelengths were 494/517 and 528/617 nm for calcein-AM and ethidium homodimer-1, respectively. The cells were imaged using a confocal microscope (LSM 800, Zeiss, Germany).

In vitro and ex vivo Drug Distribution of Cy5-NS Implant

The distribution of drug-loaded NS implants in biological samples was analyzed using pork meat and mouse livers. The Cy5-NS implant was injected into the pork meat, and the Cy5 signal was detected at the red wavelength of the fluorescence imaging device (FOBI) at pre-defined time points (0, 1, 6, and 24 h). Additionally, the Cy5-NS implant was injected into the dissected mouse liver and the Cy5 signal was detected at pre-defined time points (0, 1, and 6 h).

Biodegradation of NS Implant

The biodegradability of the NS implants was analyzed using in vivo imaging. The Cy5-NS implant was injected into the flanks of mice. The mice were observed for 7 days after injection to analyze the degradation of the Cy5-NS implant.

To evaluate degradation, ICG-NS implants were injected into the flanks of the mice. The mice were then dissected at a set time (0 and 7 days), and photographs of the remaining NS implants were taken.

In vivo Biodistribution

Tumor and organ distributions of the Cy5 solution, Cy5-NS implant, and Cy5-starch hydrogel were analyzed using in vivo imaging. 4T1 cells (1 \times 10⁶) were injected into the flanks of mice and monitored for 3 weeks. The Cy5 solution, Cy5-NS implant, and Cy5 starch hydrogel (Cy5:10 μg) were injected into the tumor, and the organ and tumor

distributions of the Cy5 signals were examined. To confirm the uniform distribution of Cy5 signals within the tumor, the tumor was divided into six pieces, and the amount of drug absorbed in each tumor piece was evaluated using *in vivo* imaging.

In vitro and in vivo Photothermal Therapy Effects

To evaluate the photothermal effect of the ICG-NS implant *in vitro*, the implant was irradiated with an NIR laser (808 nm; 1 W/cm²) for 5 min. The photothermal effect of the NS implants *in vivo* was examined after injecting 4T1 cells (1 × 10⁶) into the flanks of mice. The ICG-NS implant or 10 mM PBS (pH 7.4) solution was injected into the tumor when the tumor size reached 200–300 mm³. The tumor was irradiated with an NIR laser (808 nm, 1 W/cm²) on day 1 post injection. A photothermal camera was used to capture the thermal images.

In vivo Anti-Tumor Effects

To evaluate the anti-cancer effect of ICG-NS implants, 4T1 cells (1 × 10⁶ cells) were injected into the flanks of mice. The tumor was injected with the ICG-NS implant and PBS when the tumor size reached 200–300 mm³. Next, the tumor was irradiated with an NIR laser on day 1 post injection. The tumor size was measured once every two days. On day 14 post-treatment, the mice were euthanized and the tumors were dissected.

Statistical Analysis

All statistical analyses were performed using Microsoft Excel. Data were analyzed using a two-sample Student's *t*-test. Differences were considered significant at $P < 0.05$ (indicated with an asterisk in the figures).

Results and Discussion

Preparation and Characterization of NS Implants (Cy5-NS Implant and ICG-NS Implant)

In this study, NS implants with sufficient rigidity for injection were prepared by gelatinizing starch solution through heating. The gelatinized NS implants were dried to obtain rigid needles for injection into tumors. Starch can be molded into the desired shape and size by heating and drying in a silicone mold. The length, width, and height of the Cy5-NS implant (used for fluorescence imaging) were 1.08 ± 0.12 cm, 1.93 ± 0.2 mm, 0.93 ± 0.15 mm, respectively. And the length, width, and height of the ICG-NS implant (used for PTT) were 1.11 ± 0.21 cm, 1.97 ± 0.11 mm, and 0.88 ± 0.08 mm, respectively. Because the length of the tumor used for treatment was approximately 1 cm, the size of the needle was adjusted to approximately 1 cm using a silicone mold. The tip of the ICG-NS implant was pointed outwards, enabling easy injection into the tumor and uniform drug delivery throughout the tumor (Figure 1A–E). As this study aimed to develop a prototype of an NS implant, a simple silicone mold was used for small-scale production. Because the needle used in this experiment was a prototype, it was manufactured in small quantities manually using the silicone mold, resulting in a slight deviation in needle size. A variety of commercially available starch products, such as capsules and building materials, are engineered to the desired size and shape. Hence, any final product is expected to be uniform and mass produced cost-effectively.^{27,28}

SEM analysis was performed to examine the structure of the NS implants. Heating destroys the crystal structure of starch and induces gelatinization of the starch solution, promoting strong binding between starch molecules (Figure 2A and B-a). Recrystallization occurred during the drying process, and the dried NS implant sample showed several pores as moisture escaped from the NS implant (Figure 2A and B-b). Although the dried NS implants exhibited a perforated structure, their rigidity was sufficient for the injection. Incubation of dried starch in water for 4 h resulted in the absorption of moisture, and the starch structure transformed into a dense hydrogel form (Figure 2A and B-c). ICG-NS and Cy5-NS implants were structurally similar (Figure 2A and B).

Hydrogel systems that can absorb water are similar to biological tissues and are used in various fields (drug delivery, tissue engineering, and wound dressing). Drugs can be continuously released through the diffusion of absorbed water. Because starch is a hydrophilic substance that can absorb moisture owing to the presence of hydroxyl groups, NS implants absorb moisture and become a hydrogel. The NS implants swelled four times the initial values (based on mass

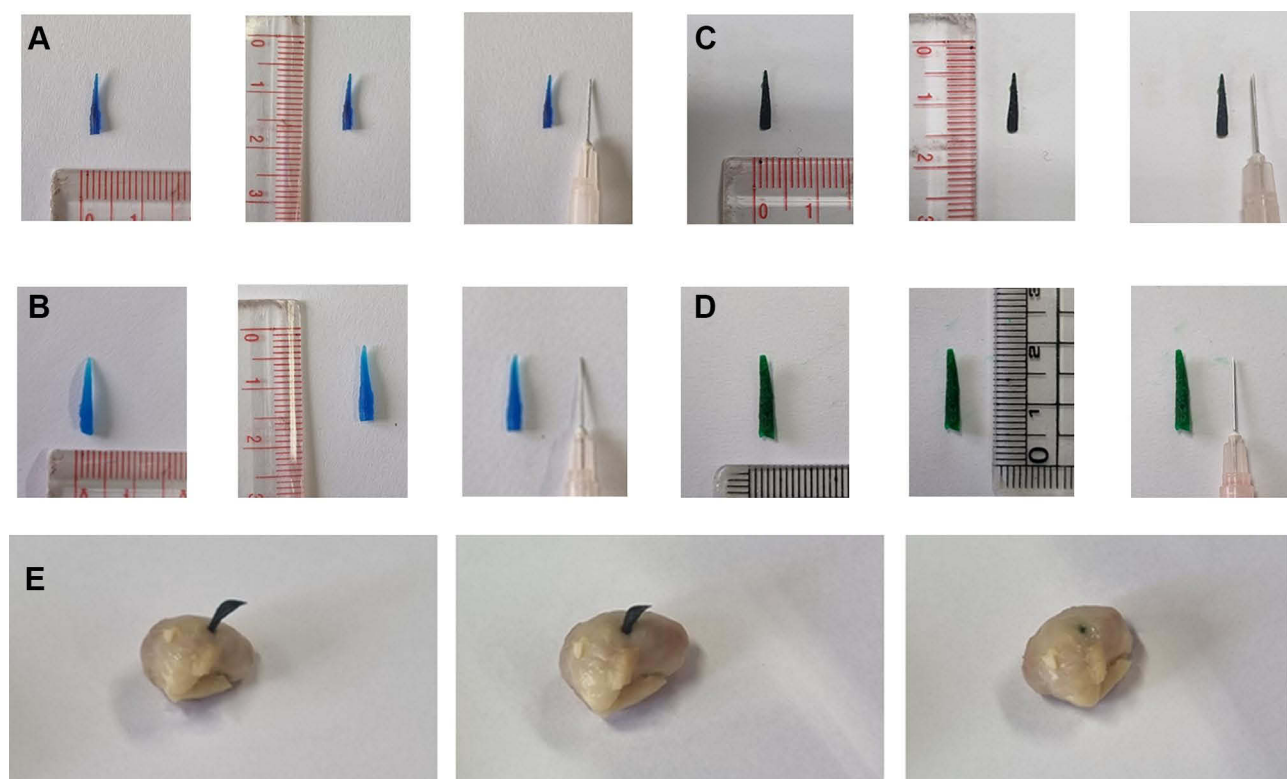


Figure 1 Images of (A) dried Cy5-NS implant, (B) Cy5-NS implant suspended in 10 mM phosphate-buffered saline PBS (pH 7.4), (C) dried ICG-NS implant, and (D) ICG-NS implant suspended in 10 mM PBS (pH 7.4). (E) Injection of ICG-NS implants into the tumors.

ratio) after incubation in water for 4 h (Figure 2C). The length and thickness of the swollen NS implants were approximately 1.2 cm and 3 mm, respectively (Figure 1B and D). These results indicate that NS implants have a hydrogel structure (which absorbs moisture) and that the drug can be loaded within this structure for continuous release.

Release Profile of ICG-NS Implant

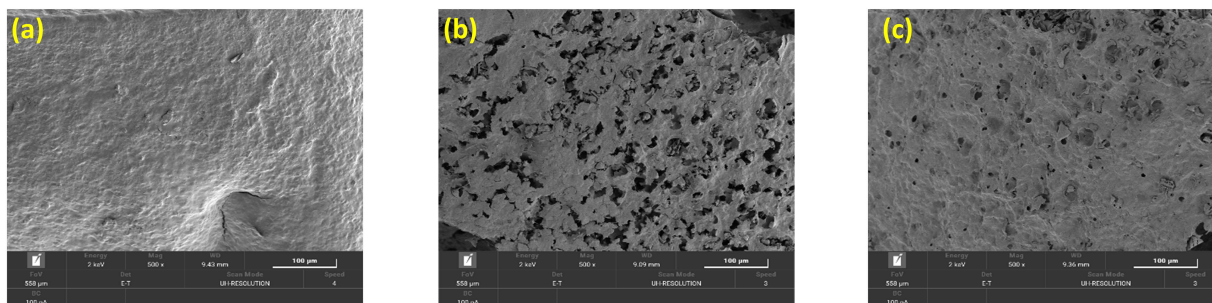
Because ICG was encapsulated in the three-dimensional structure created by gelatinization of the NS implant, the drug was continuously released for 3 days (Figure 2D). In addition, because starch can be degraded by enzymes in the body, drug release from ICG-NS implants was evaluated in PBS containing glucoamylase, an enzyme that degrades starch. Samples incubated in PBS with glucoamylase showed a faster release rate than those incubated in PBS without glucoamylase. The release rate after NIR irradiation was evaluated. In the absence of enzymes, the three-dimensional structure of starch is stable even at high temperatures; therefore, the temperature increase by NIR irradiation does not have a significant effect on the release rate. However, it was confirmed that increasing the temperature by NIR irradiation in the presence of the enzyme increased the activity of the enzyme, thereby increasing the drug release rate. Glucoamylase is an enzyme that can hydrolyze starch to glucose. In the presence of glucoamylase, the three-dimensional structure of the NS implant is destroyed by glucoamylase, allowing the encapsulated drug to be released more quickly.

As the optimal activation temperature of glucoamylase is 55 °C, the elevated temperature by NIR irradiation increases the activity of glucoamylase, leading to faster degradation of the NS implant and a sharp increase in the drug release rate.²⁹

In vitro and ex vivo Cy5 Distribution After Administration of Cy5-NS Implant

The distribution of the drug throughout the tumor after intratumoral injection is critical for therapeutic efficacy.^{9,20} Pork meat and dissected mouse livers were used as in vitro and ex vivo models, respectively, to examine the tissue distribution of the NS implant. Cyanine 5 (Cy5), which exhibits strong fluorescence, was used to confirm drug distribution in vitro and in vivo. The Cy5-NS implant (used for fluorescence imaging) could be easily injected and fixed at the target site,

A Cy5 starch needle



B ICG starch needle

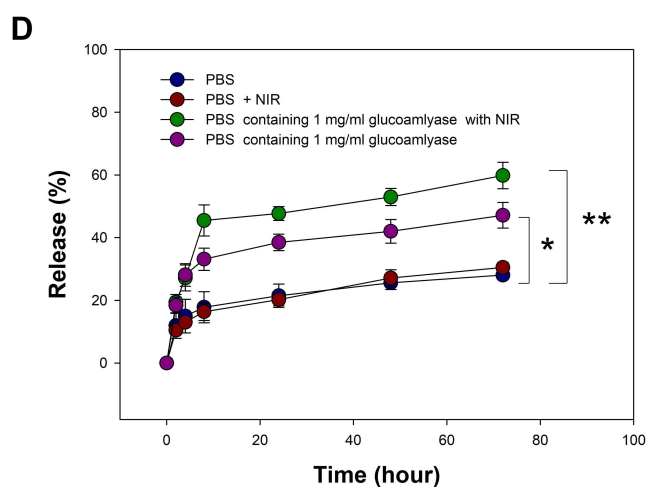
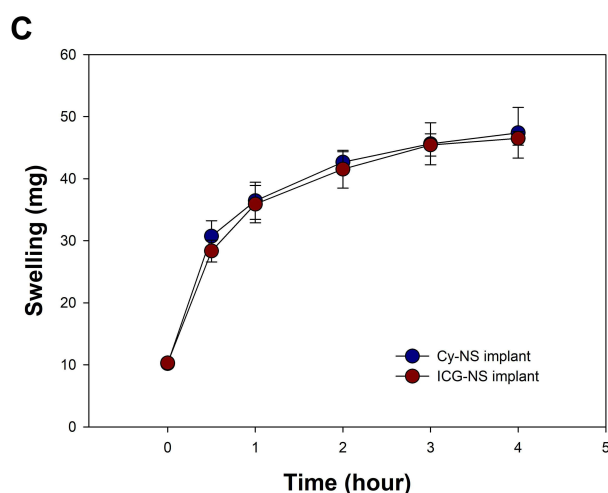
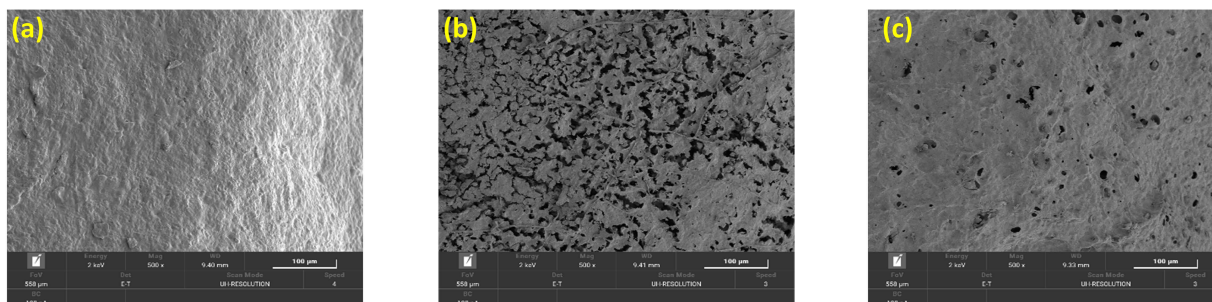


Figure 2 Scanning electron micrographs of (A) Cy5-NS implant and (B) ICG-NS implant ((a) NS implant before drying, (b) after drying, and (c) suspended in 10 mM phosphate-buffered saline (PBS pH 7.4)). (C) release profile of ICG-NS implant under different conditions (n = 3, *P < 0.05 **P < 0.01). (D) Swelling profiles of NS implant (n = 3).

enabling drug release at the injection site. Cy5-NS implants injected into the pork meat were observed for 1 d using a fluorescence imaging device. Encapsulated Cy5 was slowly released from the Cy5-starch injection site (Figure 3A and B). Analysis of the liver injected with the Cy5-NS implant revealed that the NS implant can be easily injected into the target site in vivo. The Cy5-NS implant injected into the liver was fixed at the injection site and Cy5 was continuously released from the needle to the surrounding site (Figure 3C). These results indicate that NS implants can effectively replace traditional drug delivery systems, such as solutions, hydrogels, and implants, and deliver high concentrations of drugs continuously near the injection site.

Biodegradation of NS Implant

Starch is a safe and biodegradable material that is widely used in the food industry and as a drug delivery system.^{27,30,31} Additionally, starch can be degraded by various enzymes such as amylases, glucoamylases, glucosidases, and other

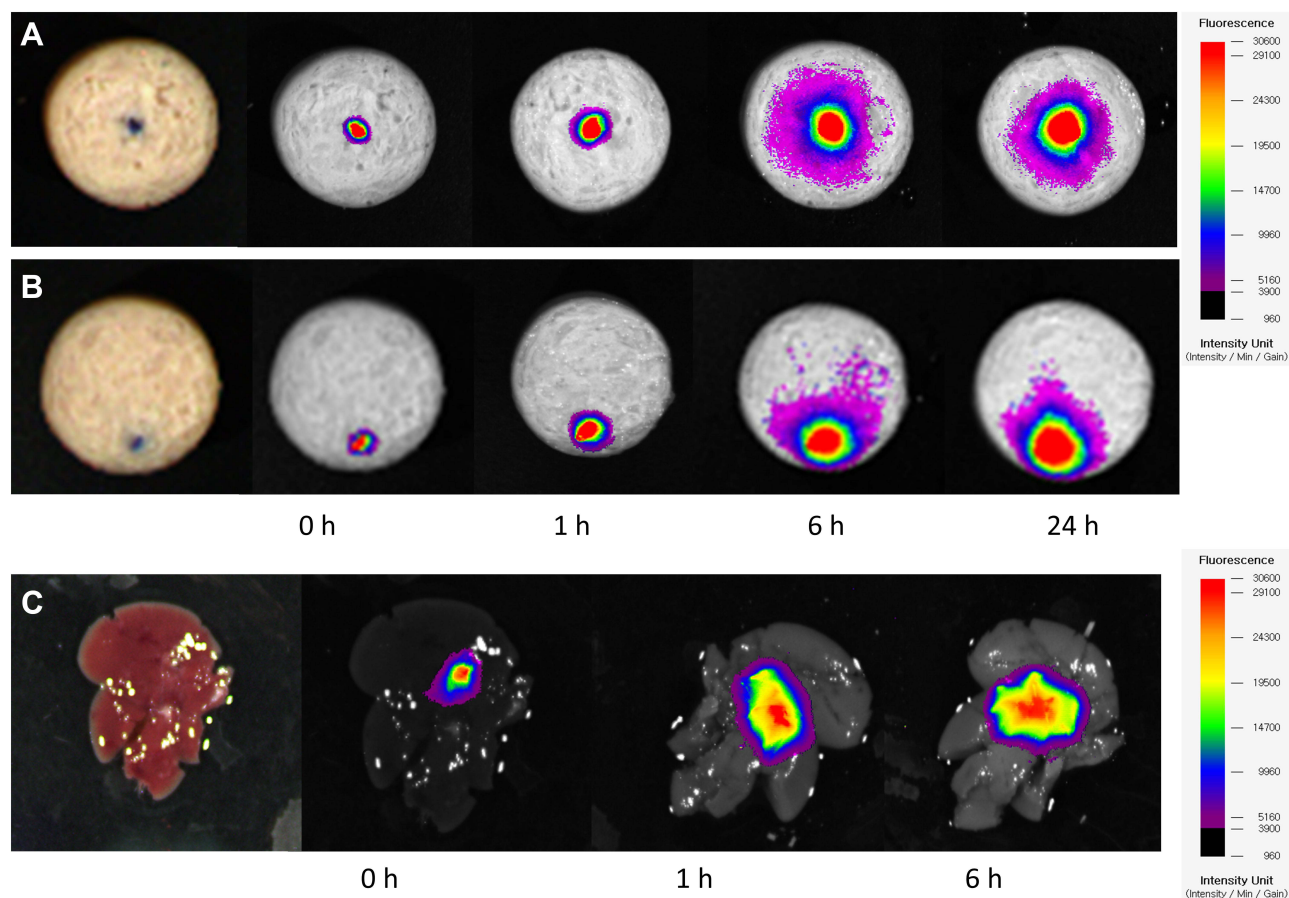


Figure 3 Fluorescence images of the (A) core and (B) lateral sites of injection in the pork meat and (C) mouse liver.

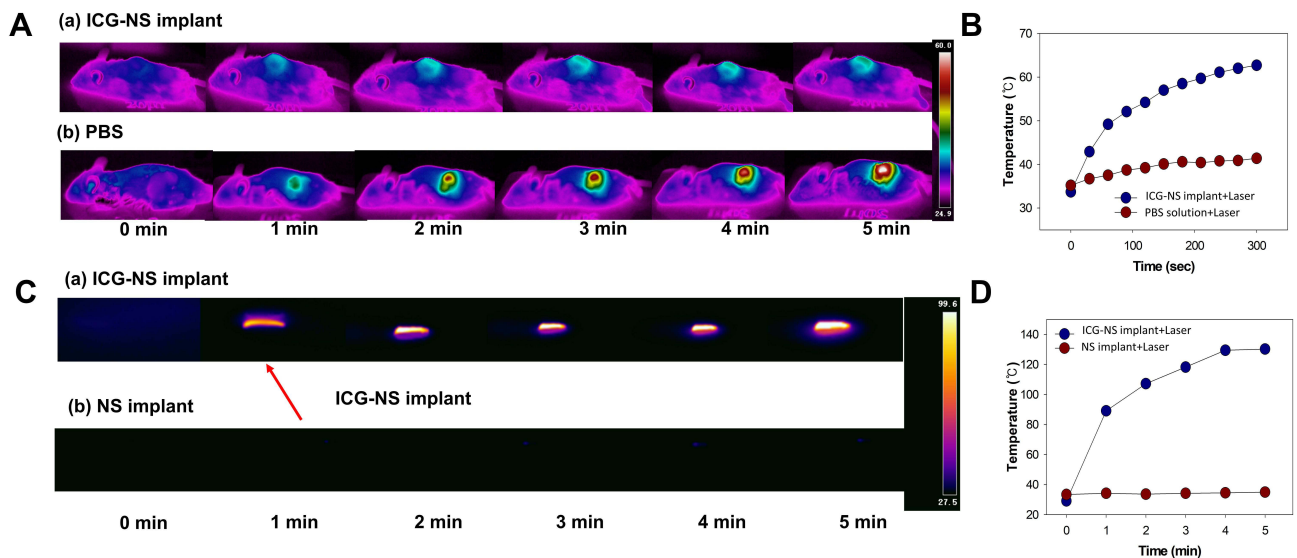
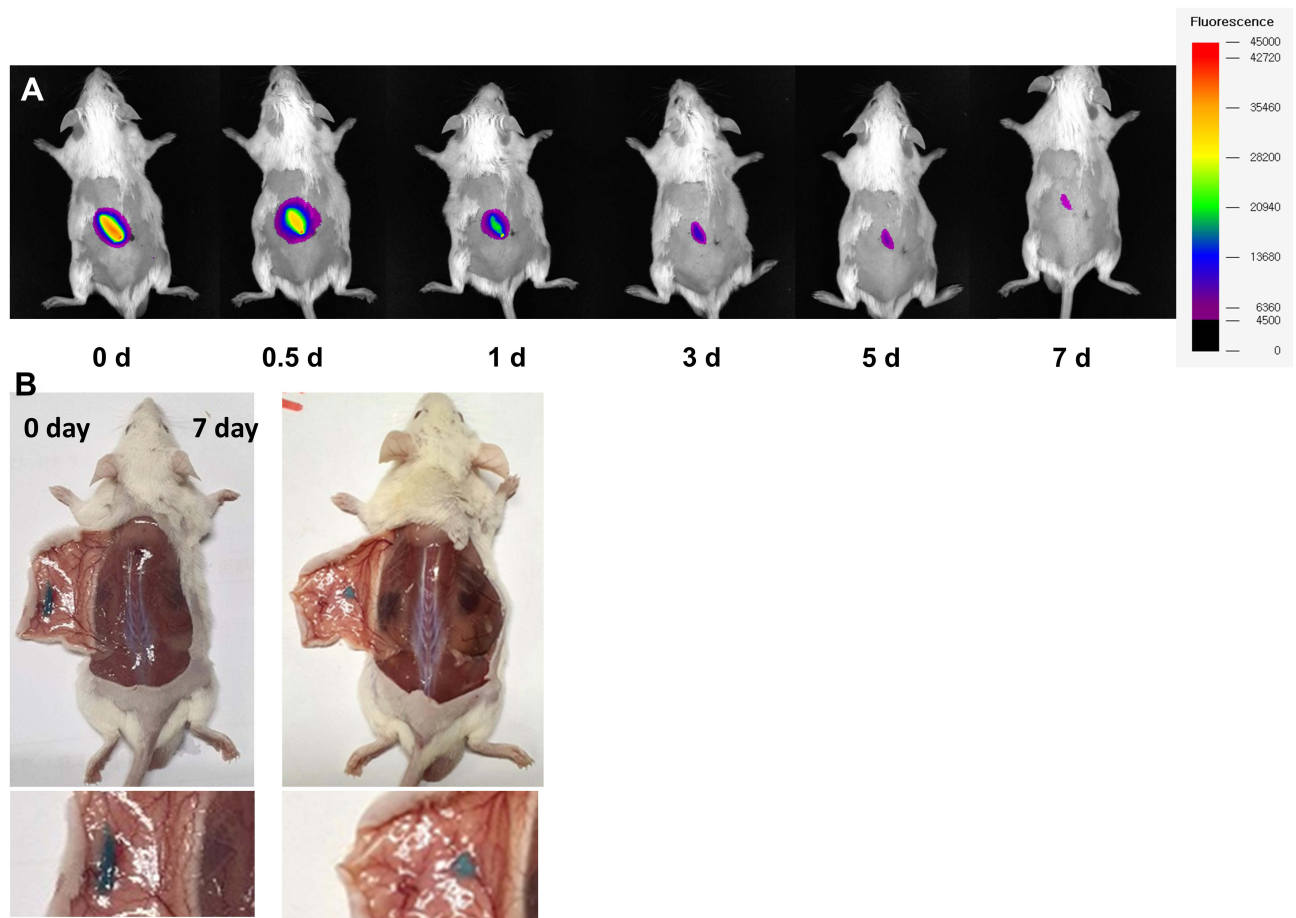
debranching enzymes. These degradation products are absorbed by the body.²⁵ Degradation of the Cy5-NS implant was observed using *in vivo* imaging and imaging of the dissected mice (Figure 4). *In vivo* imaging results confirmed that the Cy5 signal intensity in the mice administered the Cy5-NS implant continuously decreased over time. In the NS implant, Cy5 was released continuously for seven days without rapid release (Figure 4A). This indicated that Cy5 was released through the degradation of the NS implant. Figure 4B shows images taken 0 and 7 days after the injection of the ICG-NS implant. Most ICG-NS implants decomposed *in vivo* on day 7 after ICG-NS implant injection. These results indicate that the NS implants are biodegradable.

In vitro and in vivo Photothermal Effects of NS Implant

The accumulation of high concentrations of photothermal substances at the tumor site can increase photothermal effects and decrease side effects.³² In this study, the NS implant delivered a high drug concentration around the injection site *in vitro*, *ex vivo*, and *in vivo*. The ICG-NS implant enables effective photothermal treatment by delivering a high concentration of photothermal material to the desired area, particularly the tumor.

An ICG-NS implant was prepared for photothermal treatment. The *in vitro* photothermal effect of the ICG-NS implants was evaluated using an NIR laser with a wavelength of 808 nm.

The wavelength of 808 nm not only exhibits high penetration power but can also be effectively absorbed by ICG and converted into heat, making it suitable for photothermal treatment. The ICG-NS implant effectively absorbed light and increased the temperature to 130 °C in 5 min. However, the temperature of the injection site of the ICG-NS implant is expected to be below 130 °C, as the tumor absorbs some of the generated heat. Hence, the photothermal effect-mediated increase in temperature of the tumors injected with the ICG-NS implant was measured *in vivo* (Figure 5A–D).



The temperature at the site of ICG-NS implant injection in the tumor increased to $> 60\text{ }^{\circ}\text{C}$ in 5 min (Figure 5B). Photothermal therapy is an effective method to kill cancer cells. In cancer, apoptosis and necrosis occur at temperatures above $41\text{ }^{\circ}\text{C}$ and $50\text{ }^{\circ}\text{C}$, respectively.³³ This indicates that ICG-NS implants are suitable for photothermal treatment, which can kill tumors.

In vitro Cytotoxicity

The effect of NIR laser irradiation on the viability of 4T1 cells was evaluated using an MTT assay. As shown in Figure 6A, the ICG-NS and NS implants did not exert cytotoxic effects on unirradiated cells. In addition, the NS implants without NIR laser irradiation did not show any cytotoxic effects. In contrast, ICG-NS implants with NIR laser irradiation decreased cell viability to less than 10%. The live/dead assay results were similar to those of the MTT assay (Figure 6B). 4T1 cells treated with ICG-NS implant with NIR laser irradiation showed strong red fluorescence, indicating that they were mostly dead cells. The other treatment groups showed only strong green fluorescence, indicative of live cells.

These results indicate that ICG encapsulated in the ICG-NS implant effectively absorbs light energy from the laser, converts it into heat energy, and consequently exerts antitumor effects.

In vivo Biodistribution

In this study, the Cy5-starch hydrogel, Cy5-NS implant, and Cy5 solution were injected into 4T1 tumors. The distribution of the drugs within the tumors and organs was analyzed (Figure 7). Cy5 was slowly released from the Cy5-starch hydrogel and Cy5-NS implant, and only a small amount of Cy5 was absorbed into the organs at 10 min and 1 d post-injection. However, Cy5 delivered through a solution was rapidly absorbed into the body and distributed between the organs, including the liver and kidneys (Figure 7A). Large amounts of Cy5 were distributed in the tumors after administration of Cy5 or Cy5-NS implants. In the case of the Cy5-hydrogel, a high concentration of Cy5 was observed only in the tumor area around the hydrogel at 10 min and 1 d post-injection (Figure 7B).

To analyze the uniform distribution of the drug within the tumor, the tumor was divided into six sections and analyzed. Cy5 delivered through the NS implant was more uniformly distributed throughout the tumor than that delivered through the solution or starch hydrogel. The Cy5-NS implant enabled the maintenance of a high drug concentration even 1 d post-treatment (Figure 7C). Comparative analysis of the distribution of Cy5 delivered through the NS implant and starch hydrogel revealed that the precise injection site inside the tumor plays an important role in the uniform drug

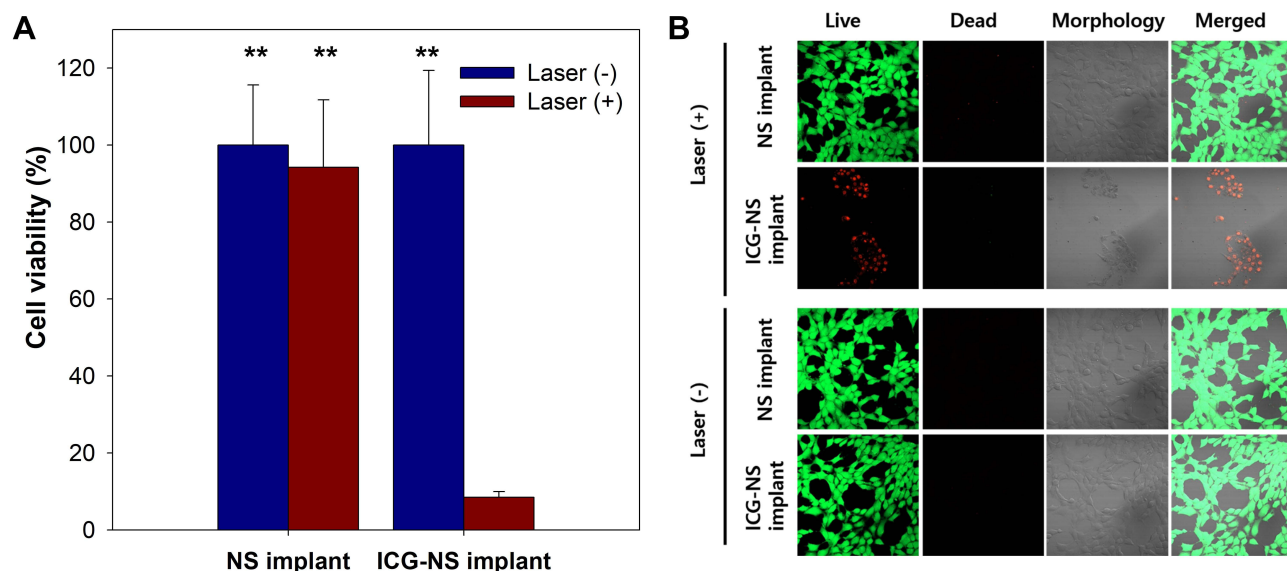


Figure 6 (A) In vitro cytotoxic effects of ICG-NS implant with near-infrared (NIR) laser (808 nm , $1\text{ W}/\text{cm}^2$ for 5 min)-irradiated and unirradiated 4T1 cells ($n = 8$, $**P < 0.01$ compared to ICG-NS implant with laser). (B) Live/Dead assay of 4T1 cells treated with NS implant, ICG-NS implant with and without irradiation with laser light (808 nm , $1\text{ W}/\text{cm}^2$ for 5 min).

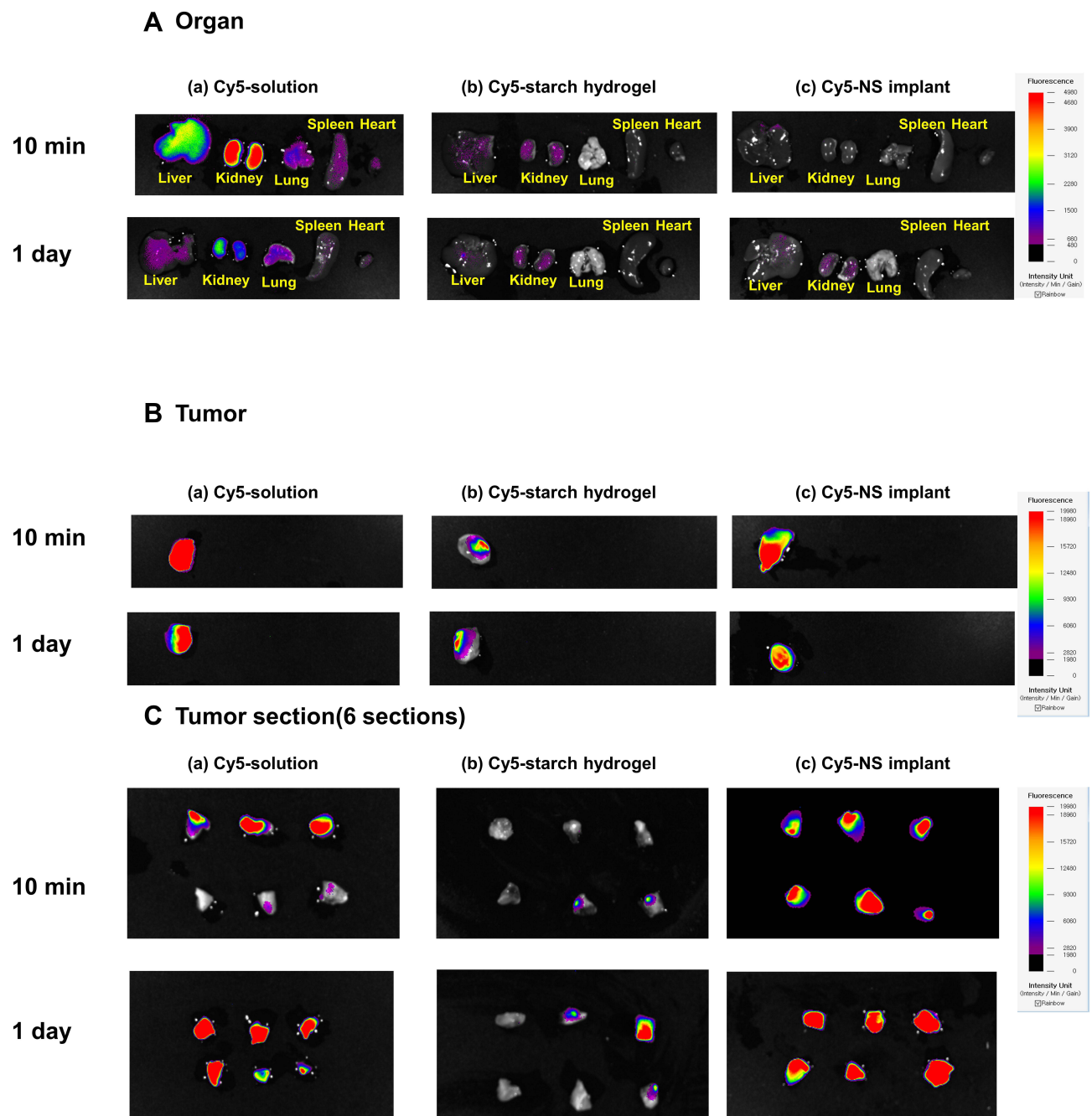


Figure 7 In vivo fluorescence imaging of the (A) organs (liver, kidney, lung, spleen, and heart), (B) tumor, and (C) tumor sections (6 sections).

distribution within the tumor. In vivo imaging analysis of intratumoral drug distribution revealed that the NS implant could continuously and uniformly deliver the drug to the tumor and reduce the amount of drug absorbed into the organ.

In vivo Photothermal Anti-Tumor Effects

4T1 tumor-bearing mice were used to evaluate the photothermal effects of ICG-NS implants in vivo. The mice were administered the ICG-NS implant or PBS when the tumor size reached 200–300 mm³. One day later, the tumor was subjected to laser irradiation. The cytotoxicity of the NS implant was evaluated by examining the growth of tumors that were irradiated or not irradiated with the NIR laser (Figure 8). NIR laser irradiation effectively inhibited the growth of ICG-NS implant-treated tumors (tumor size less than 100 mm³). In contrast, ICG-NS implants or PBS did not inhibit

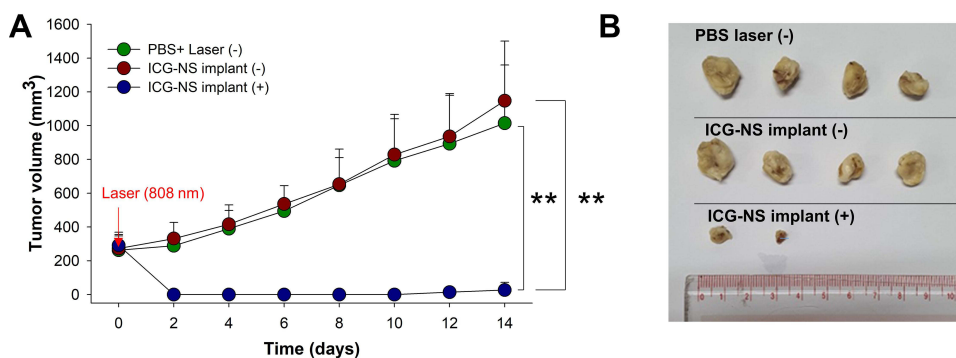


Figure 8 (A) Tumor size in 4T1 tumor-bearing mice treated with phosphate-buffered saline (PBS) and ICG-NS implant in the presence or absence of near-infrared laser irradiation (808 nm, 1 W/cm² for 5 min). **(B)** Photographs of 4T1 tumors resected from mice after treatment (n = 4, **P < 0.01).

tumor growth (tumor size > 1000 mm³) in the absence of NIR laser irradiation. This indicated that the ICG-NS implant exhibited antitumor activity through the photothermal effect.

Conclusion

In this study, a needle-type starch implant was developed that can be easily injected into a tumor. Drug-encapsulated implants are prepared with the desired size and shape using starch gelatinization and drying processes. In addition, a needle with sufficient rigidity was injected into the tumor core without any special equipment or procedures, and the drug was continuously released throughout the tumor. Compared with the conventional intratumoral injection method, NS implants have reduced systemic absorption, enabling high-concentration drug delivery within the tumor. As NS implants can deliver high concentrations of photothermal substances to tumors, they can exhibit an effective anticancer inhibitory effect through PTT. Intratumoral administrable needle-type starch implants are expected to be a new strategy for effective drug delivery to tumors.

Acknowledgments

This research was supported by the Basic Science Research Program through the National Research Foundation of Korea (NRF) funded by the Ministry of Education (2021R1F1A1047799).

Disclosure

Professor Changkyu Lee reports a patent 10-2021-0147836 pending. The author reports no other conflicts of interest in this work.

References

1. Yu Z, Gao L, Chen K, et al. Nanoparticles: a new approach to upgrade cancer diagnosis and treatment. *Nanoscale Res Lett.* 2021;16(1):88. doi:10.1186/s11671-021-03489-z
2. Zhao L, Zhang X, Wang X, Guan X, Zhang W, Ma J. Recent advances in selective photothermal therapy of tumor. *J Nanobiotechnology.* 2021;19(1):335. doi:10.1186/s12951-021-01080-3
3. Pham PTT, Le XT, Kim H, et al. Indocyanine green and curcumin co-loaded nano-fireball-like albumin nanoparticles based on near-infrared-induced hyperthermia for tumor ablation. *Int J Nanomedicine.* 2020;15:6469–6484. doi:10.2147/IJN.S262690
4. Pan H, Zhang C, Wang T, Chen J, Sun SK. In situ fabrication of intelligent photothermal indocyanine green-alginate hydrogel for localized tumor ablation. *ACS Appl Mater Interfaces.* 2019;11(3):2782–2789. doi:10.1021/acsami.8b16517
5. Sitia L, Sevieri M, Bonizzi A, et al. Development of tumor-targeted indocyanine green-loaded ferritin nanoparticles for intraoperative detection of cancers. *ACS Omega.* 2020;5(21):12035–12045. doi:10.1021/acsomega.0c00244
6. Dai Q, Wilhelm S, Ding D, et al. Quantifying the ligand-coated nanoparticle delivery to cancer cells in solid tumors. *ACS nano.* 2018;12(8):8423–8435. doi:10.1021/acsnano.8b03900
7. Wilhelm S, Tavares AJ, Dai Q, et al. Analysis of nanoparticle delivery to tumours. *Nat Rev Mater.* 2016;1(5):1–12. doi:10.1038/natrevmats.2016.14
8. Yang Y, Qiao X, Huang R, et al. E-jet 3D printed drug delivery implants to inhibit growth and metastasis of orthotopic breast cancer. *Biomaterials.* 2020;230:119618. doi:10.1016/j.biomaterials.2019.119618
9. Marabelle A, Andtbacka R, Harrington K, et al. Starting the fight in the tumor: expert recommendations for the development of human intratumoral immunotherapy (HIT-IT). *Ann Oncol.* 2018;29(11):2163–2174. doi:10.1093/annonc/mdy423
10. Park SH, Panta P, Heo JY, et al. An intratumoral injectable, electrostatic, cross-linkable curcumin depot and synergistic enhancement of anticancer activity. *NPG Asia Mater.* 2017;9(6):e397–e397. doi:10.1038/am.2017.102

11. Melero I, Castanon E, Alvarez M, Champiat S, Marabelle A. Intratumoural administration and tumour tissue targeting of cancer immunotherapies. *Nat Rev Clin Oncol*. 2021;18:1–19. doi:10.1038/s41571-020-00441-5
12. Shemi A, Khvalevsky EZ, Gabai RM, Domb A, Barenholz Y. Multistep, effective drug distribution within solid tumors. *Oncotarget*. 2015;6(37):39564–39577. doi:10.18632/oncotarget.5051
13. Eikenes L, Tari M, Tufto I, Bruland ØS, de Lange Davies C. Hyaluronidase induces a transcapillary pressure gradient and improves the distribution and uptake of liposomal doxorubicin (Caelyx™) in human osteosarcoma xenografts. *Br J Cancer*. 2005;93(1):81–88. doi:10.1038/sj.bjc.6602626
14. Cui R, Wu Q, Wang J, et al. Hydrogel-by-design: smart delivery system for cancer immunotherapy. *Front Bioeng Biotechnol*. 2021;671. doi:10.3389/fbioe.2021.723490
15. Fan DY, Tian Y, Z-j L. Injectable hydrogels for localized cancer therapy. *Front Chem*. 2019;7:675. doi:10.3389/fchem.2019.00675
16. Yang Y, Wang F, Zheng K, et al. Injectable PLGA/Fe3O4 implants carrying cisplatin for synergistic magnetic hyperthermal ablation of rabbit VX2 tumor. *PLoS One*. 2017;12(5):e0177049. doi:10.1371/journal.pone.0177049
17. Yu T, Liu K, Wu Y, et al. High interstitial fluid pressure promotes tumor cell proliferation and invasion in oral squamous cell carcinoma. *Int J Mol Med*. 2013;32(5):1093–1100. doi:10.3892/ijmm.2013.1496
18. Chu X-Y, Huang W, Wang Y-L, et al. Improving antitumor outcomes for palliative intratumoral injection therapy through lecithin–chitosan nanoparticles loading paclitaxel–cholesterol complex. *Int J Nanomedicine*. 2019;14:689. doi:10.2147/IJN.S188667
19. Muñoz NM, Williams M, Dixon K, et al. Influence of injection technique, drug formulation and tumor microenvironment on intratumoral immunotherapy delivery and efficacy. *J Immunother Cancer*. 2021;9(2):e001800. doi:10.1136/jitc-2020-001800
20. Boone CE, Wang C, Lopez-Ramirez MA, et al. Active microneedle administration of plant virus nanoparticles for cancer in situ vaccination improves immunotherapeutic efficacy. *Acs Appl Nano Mater*. 2020;3(8):8037–8051. doi:10.1021/acsnm.0c01506
21. Waghule T, Singhvi G, Dubey SK, et al. Microneedles: a smart approach and increasing potential for transdermal drug delivery system. *Biomed Pharmacother*. 2019;109:1249–1258. doi:10.1016/j.biopha.2018.10.078
22. Ashby LS, Smith KA, Stea B. Gliadel wafer implantation combined with standard radiotherapy and concurrent followed by adjuvant temozolomide for treatment of newly diagnosed high-grade glioma: a systematic literature review. *World J Surg Oncol*. 2016;14. doi:10.1186/s12957-016-0975-5
23. Nagano S, Yokouchi M, Setoguchi T, et al. Analysis of surgical site infection after musculoskeletal tumor surgery: risk assessment using a new scoring system. *Sarcoma*. 2014;2014:1–9. doi:10.1155/2014/645496
24. Troncoso OP, Torres FG. Non-conventional starch nanoparticles for drug delivery applications. *Med Devices Sens*. 2020;3(6):e10111. doi:10.1002/mds3.10111
25. Gopinath V, Saravanan S, Al-Maleki A, Ramesh M, Vadivelu J. A review of natural polysaccharides for drug delivery applications: special focus on cellulose, starch and glycogen. *Biomed Pharmacother*. 2018;107:96–108. doi:10.1016/j.biopha.2018.07.136
26. Wang R, Chen C, Guo S. Effects of drying methods on starch crystallinity of gelatinized foxtail millet (α -millet) and its eating quality. *J Food Eng*. 2017;207:81–89. doi:10.1016/j.jfoodeng.2017.03.018
27. Zhang Y, Wu M, Tan D, et al. A dissolving and glucose-responsive insulin-releasing microneedle patch for type 1 diabetes therapy. *Journal of Materials Chemistry B*. 2021;9(3):648–657. doi:10.1039/D0TB02133D
28. Biduski B, da Silva WMF, Colussi R, et al. Starch hydrogels: the influence of the amylose content and gelatinization method. *Int J Biol Macromol*. 2018;113:443–449. doi:10.1016/j.ijbiomac.2018.02.144
29. Mishra A, Debnath M. Effect of pH on simultaneous saccharification and isomerization by glucoamylase and glucose isomerase. *Appl Biochem Biotech*. 2002;102:193–199. doi:10.1385/Abab:102-103:1-6:193
30. Wang HY, Jiang LM, Wu HH, et al. Biocompatible iodine-starch-alginate hydrogel for tumor photothermal therapy. *Acs Biomater Sci Eng*. 2019;5(7):3654–3662. doi:10.1021/acsbomaterials.9b00280
31. Li Y, Hu H, Zhou Q, et al. α -Amylase-and redox-responsive nanoparticles for tumor-targeted drug delivery. *ACS Appl Mater Interfaces*. 2017;9(22):19215–19230. doi:10.1021/acsmi.7b04066
32. Liu Y, Mo F, Hu J, et al. Precision photothermal therapy and photoacoustic imaging by in situ activatable thermoplasmonics. *Chem Sci*. 2021;12:10097
33. Lee C, Kang S. Development of HER2-targeting-ligand-modified albumin nanoparticles based on the SpyTag/SpyCatcher system for photothermal therapy. *Biomacromolecules*. 2021;22:2649–2658. doi:10.1021/acs.biomac.1c00336

International Journal of Nanomedicine

Dovepress

Publish your work in this journal

The International Journal of Nanomedicine is an international, peer-reviewed journal focusing on the application of nanotechnology in diagnostics, therapeutics, and drug delivery systems throughout the biomedical field. This journal is indexed on PubMed Central, MedLine, CAS, SciSearch®, Current Contents®/Clinical Medicine, Journal Citation Reports/Science Edition, EMBase, Scopus and the Elsevier Bibliographic databases. The manuscript management system is completely online and includes a very quick and fair peer-review system, which is all easy to use. Visit <http://www.dovepress.com/testimonials.php> to read real quotes from published authors.

Submit your manuscript here: <https://www.dovepress.com/international-journal-of-nanomedicine-journal>